# Computational Investigation of Turbulent Swirling Flows in Gas Turbine Combustors

**A. C. Benim[1], M. P. Escudier[2], P. J. Stopford[3], E. Buchanan[4] and K. J. Syed[4]**

[1]Department of Mechanical and Process Engineering, Duesseldorf University of Applied Sciences
Josef-Gockeln-Str. 9, D-40474 Duesseldorf, Germany
[2]Department of Engineering, University of Liverpool,
Chadwick Building, Peach Street, Liverpool L69 3GH, UK
[3]ANSYS Europe Ltd., West Central 127, Milton Park, Abingdon, Oxfordshire, OX14 4SA, UK
[4]Combustor Development, Siemens Industrial Turbomachinery Ltd.
PO Box 1, Waterside South, Lincoln LN5 7FD, UK

## Abstract

In the first part of the paper, Computational Fluid Dynamics analysis of the combusting flow within a high-swirl lean premixed gas turbine combustor and over the 1st row nozzle guide vanes is presented. In this analysis, the focus of the investigation is the fluid dynamics at the combustor/turbine interface and its impact on the turbine. The predictions show the existence of a highly-rotating vortex core in the combustor, which is in strong interaction with the turbine nozzle guide vanes. This has been observed to be in agreement with the temperature indicated by thermal paint observations. The results suggest that swirling flow vortex core transition phenomena play a very important role in gas turbine combustors with modern lean-premixed dry low emissions technology. As the predictability of vortex core transition phenomena has not yet been investigated sufficiently, a fundamental validation study has been initiated, with the aim of validating the predictive capability of currently-available modelling procedures for turbulent swirling flows near the sub/supercritical vortex core transition. In the second part of the paper, results are presented which analyse such transitional turbulent swirling flows in two different laboratory water test rigs. It has been observed that turbulent swirling flows of interest are dominated by low-frequency transient motion of coherent structures, which cannot be adequately simulated within the framework of steady-state RANS turbulence modelling approaches. It has been found that useful results can be obtained only by modelling strategies which resolve the three-dimensional, transient motion of coherent structures, and do not assume a scalar turbulent viscosity at all scales. These models include RSM based URANS procedures as well as LES and DES approaches.

**Keywords**: Turbulent swirling flows, gas turbine combustors, URANS, RSM, LES, DES

## 1. Introduction

Turbine design processes have evolved over decades and are capable of yielding very good preliminary designs due to the large amount of empirical input and experience that they embody. The empiricism which underpins the turbine design process is largely based upon experience gained on conventional non-premixed combustor applications. Lean premixed combustors, however, exhibit flows that can be substantially different from non-premixed ones, due to a significantly greater degree of swirl acquired by the flow. High swirl is required because the flow reversal through vortex breakdown is the favoured method of flame stabilisation. Additionally, a large proportion of the combustor air is swirled in order to ensure a lean premixed reaction zone. An example of such a combustor is the dry low emissions (DLE) combustor of Siemens Industrial Turbines [1], which is considered in the present paper.

A vortex breakdown along the swirl axis can be thought of as an abrupt transition between an upstream super-critical flow and a downstream sub-critical flow [2]. The criticality of the swirling flow describes whether the axial flow velocity exceeds the relative phase velocity of upstream-directed inertia waves (super-critical) or vice versa (sub-critical). The influence of the downstream conditions can hence be transmitted upstream where the flow is sub-critical, but only affects the local flow at the exit where it is super-critical. The criticality of the flow is dependent on, for example, the ratio of the swirl to axial velocity. The larger this ratio,

the higher is the tendency for sub-critical flow to occur.

A post-vortex breakdown sub-critical flow can revert to super-critical as a result of an axial acceleration of the flow. In practical gas turbine combustors the swirl is relatively high in order to ensure good fluid dynamic and combustion stability, such that in the absence of combustion, the vortex core typically remains sub-critical downstream of the vortex breakdown. However, in the case of combustion, volumetric expansion produces an increase in axial velocity due to mass continuity, whilst the tangential velocity remains more or less unchanged. This can lead to a transition to super-critical flow, making the combustor flow field relatively insensitive to downstream conditions. However, whether or not the flow reverts to super-critical, will clearly depend upon the degree of initial swirl and the density ratio between the inlet flow and the hot combustion products, as well as radial variation of velocities, pressure and density and turbulence, etc.. In dry low emissions gas turbine combustors, the flame temperatures are rather low, which may weaken the mechanism of transition to super-critical flow via axial flow acceleration. If the flow remains sub-critical, the strong acceleration in the turbine nozzle guide vanes downstream of the combustor could lead to high rotational velocities of the vortex core that can impact the turbine aerodynamic and heat transfer performance. A quantitative predictive method for addressing such flows is therefore of great importance to combustor design.

Although many analytical and numerical investigations have been conducted to address vortex breakdown and the criticality of the vortex core [3-6] much of this work is based upon simplifying assumptions, such as axisymmetry in conjunction with a Reynolds Averaged Navier-Stokes (RANS) based turbulence modelling. These studies have revealed much about the behaviour of vortical flows but they fall short of delivering quantitative information that can be used in the design of combustors, since low-frequency transient motion of coherent structures, which can play a very important role in swirling flows, cannot be represented adequately by a RANS based turbulence modelling approach.

In the first part of the paper, it is demonstrated that very encouraging results can indeed be obtained for a high-swirl lean premixed gas turbine combustor flow, which qualitatively agree with the measurements [7], applying an Unsteady RANS (URANS) based turbulence modelling approach, utilizing a Reynolds Stress Model (RSM) as the statistical turbulence model.

If computational methods are to be used effectively in the design of swirl combustors, validation is required to understand the impact of the numerical and modelling deficiencies. This is addressed in the second part of the study. Turbulent swirling flows are investigated in water test rigs that resemble gas turbine combustor configurations, experimentally and computationally, using RSM based URANS, Large Eddy Simulations (LES) and Detached Eddy Simulations (DES).

## 2. Modelling

The analysis has been based on the commercial general-purpose CFD software ANSYS-CFX [8]. It is already known [9] that certain Reynolds stress components are significantly modified due to the action of flow curvature and pressure gradient within swirling flows. Thus, eddy viscosity models, which do not address such phenomena, perform badly. Such phenomena can however be accommodated within a Reynolds stress model (RSM) closure [10]. In our experience, transient coherent flow structures can constitute an equally-important phenomenon for many types of turbulent swirling flows, and also need to be adequately modelled. Thus, modelling procedures that simultaneously account for both of these phenomena are considered in the present work. Since the transience is intimately related with three-dimensionality, a fully three-dimensional modelling is required. For the turbulent flow, the following modelling approaches are currently being investigated:

URANS-RSM: Unsteady RANS analysis based on the RSM formulation of Speziale et al. [11], applying a quadratic correlation for the isotropisation of production in the pressure-strain tensor. LES: Large Eddy Simulations [12], modelling the subgrid dissipation by a subgrid scale eddy viscosity proposed by Smagorinsky [13]. For the model coefficient, a constant value of 0.1 is used ($C_S$=0.1). The Van Driest damping function [14] is used for computing the subgrid scale viscosity in the vicinity of solid boundaries. DES: Detached Eddy Simulations [15,16], as a LES-RANS hybrid modelling approach. In the present application, the model is based on the Shear Stress Transport (SST) model of Menter [17] as the background RANS model.

Near solid walls, the wall-functions approach is used [8] for modelling the near-wall turbulence. Although the underlying assumptions are less justifiable in conjunction with the present modelling strategies, particularly with LES, it is assumed that no substantial drawbacks would result, since the major characteristics of the presently investigated flow are of free-shear type rather being wall-induced.

In combusting flow applications, mixing and reaction of the oxidant and fuel are simulated by the Eddy Dissipation Concept (EDC) of Magnussen and Hjertager [18]. The oxidation of the natural gas fuel, which is assumed to be 100% methane with the correct heat input, is represented by a two-step global reaction mechanism of Westbrook and Dryer [19].

In LES computations the convection terms are discretized by central differencing. In URANS-RSM computations, the high resolution scheme is used for the momentum equations. In DES, the central differencing is used for momentum equations in LES regions, whereas the high resolution scheme is used in RANS regions. For the turbulence quantities, the upwind scheme is used.

For the temporal discretization a second order backward Euler scheme is applied [8]. For LES and DES computations, the time-step size is chosen to be of similar magnitude with the Kolmogorov time scale [20] and results in cell Courant numbers [21] smaller than unity. For the URANS-RSM computations, larger time-step sizes are sometimes used, but these are still small enough sufficiently resolve the eddy turnover time.

## 3. Results

### 3.1 Dry Low Emissions Combustor

For the analysis of the Dry Low Emissions Gas Turbine Combustor, the URANS-RSM methodology is has been applied. An unstructured grid consisting of tetrahedral cells is used to discretize the computational domain. The solution domain is defined to include the combustor and the nozzle guide vanes at the exit of the combustor.

Instantaneous velocity vector field in a longitudinal plane in the combustor front end is displayed in Fig. 1. The vectors are coloured by the velocity magnitude. The displayed velocity vector field reveals the transient nature of the flow field, which exhibits a complex internal recirculation zone (vortex breakdown), and a precessing vortex core.
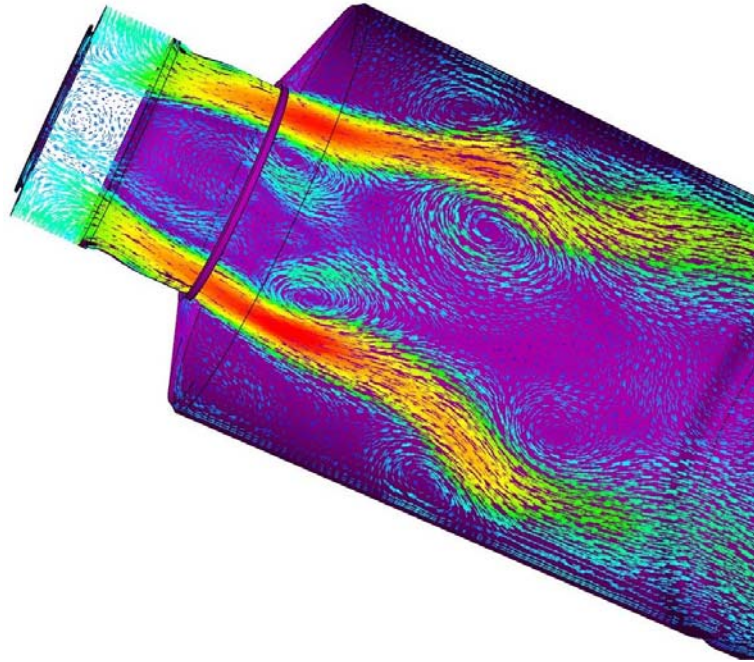


**Fig. 1** Instantaneous velocity vector field in a longitudinal plane near the combustor inlet.

Figure 2 shows the temperature distribution in a longitudinal plane, as well as an iso-surface of high vorticity. The latter, which is normally known to be high in boundary layers and shear layers, can also be high in the central part of a Rankine-type vortex, which exhibits a solid body rotation. Moving away from the centre of the vortex, the vorticity magnitude drops, given that the outer potential vortex is irrotational. A highly-rotating vortex core is indicated along the axis of the combustor. In Fig. 2, one can observe that the vortex core extends all the way through the combustor axis and intensively interacts with the nozzle guide vanes. By this interaction, the cooling aerodynamics of the nozzle guide vanes may get substantially disturbed, and, given that the vortex core is additionally very hot, the nozzle guide vanes may get excessively overheated. In such cases, it is observed that the predictions are in an excellent qualitative agreement with the experimental observations [7].
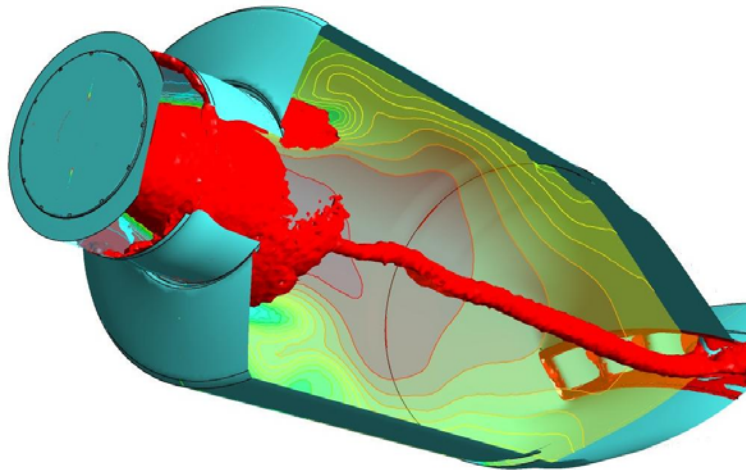


**Fig. 2** Temperature contours (yellow) in a longitudinal plane and iso-surface of high vorticity (red).

**3.2 Water Test Rig I**

A sketch of the water test rig of Escudier and Keller [22] is shown in Fig. 3. A tangential velocity component is imparted to the inflowing water by an array of 32 guide vanes. The radially-inflowing swirling flow is channeled by an axial annular duct to the main test section, which will be referred to hereafter as the "combustor". The rig operates at Re=7000 (Reynolds number is based on the diameter and the bulk axial velocity of the combustor). Measurements were performed by Laser Doppler Anemometry (LDA). Different swirl levels were obtained by adjusting the swirler guide vanes angles. The variable exit contraction enables the investigation of downstream conditions on the upstream flow, depending on whether the flow is sub- or super-critical.
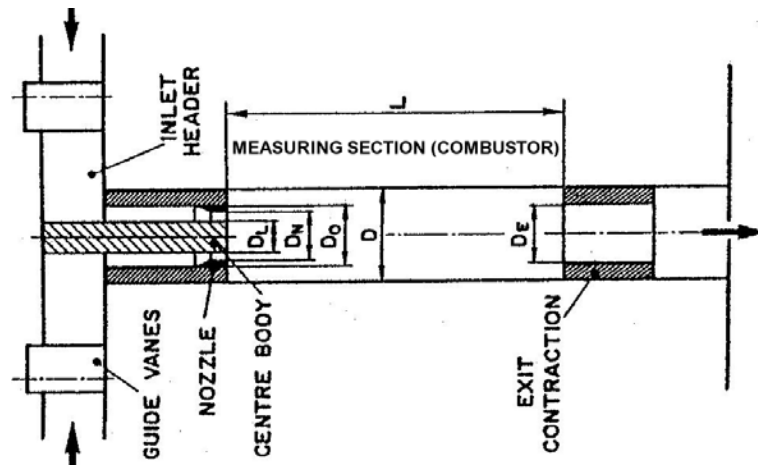
**Fig. 3** Water test rig I [22].

Measurements were provided for two swirl levels, corresponding to guide vane angles ($\alpha$) 62° and 70°. The swirl number, based on the potential theory, took the values 2.74 ($\alpha=62°$) and 11.80 ($\alpha=70°$). In addition to measurements with no exit contraction, various exit area contractions were considered. In the present work, the case with $\alpha=62°$, without exit contraction is discussed. The solution domain is defined to start in the annular channel, slightly upstream of the combustor. Preliminary 3D RANS computations were performed for a domain covering the guide vanes of the swirl generator and the axial inlet channel. In the main computations, the block-structured grid with conformal block interfaces consisted of approximately 600,000 hexa cells.

Detail plots of the velocity field, for an instant in time, in a longitudinal section near the inlet, as predicted by URANS – RSM, LES and DES are shown in Fig. 4. The smallest eddy structures seem to be captured by LES, whereas URANS – RSM resolves the largest structures, as expected.
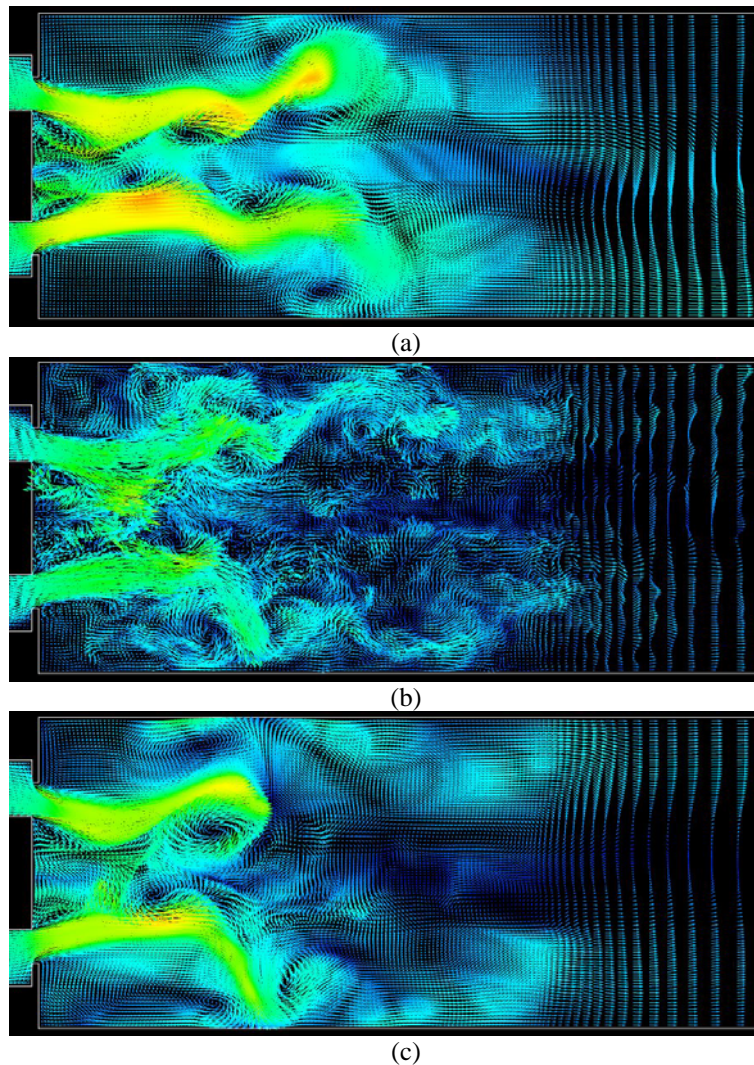


(a)



(b)



(c)

**Fig. 4** Predicted instantaneous velocity vector field in a longitudinal plane, near inlet: (a) URANS-RSM, (b) LES, (c) DES.

For the time-averaged Internal Recirculation Zone (IRZ), a quantitative comparison with the experimental data is provided in Table I, where the predicted radial (r) and axial (x) extensions of the IRZ (non-dimensionalized by combustor radius R) are compared with the experimental values.

Table I shows that the same radial extension is predicted for the IRZ, by the URANS – RSM and DES models, which underpredict the measurement by approx. 13%. For the axial extent of the IRZ, DES shows an even better agreement with the experiments. LES overpredicts the radial extent of the IRZ approximately by 17%, while it cannot predict the closure of the IRZ.

**Table I.** Radial and axial extensions of the IRZ.

|  | Exp. | U-RSM | LES | DES |
|---|---|---|---|---|
| r/R | 0.48 | 0.42 | 0.56 | 0.42 |
| x/R | 2.88 | 3.49 | unclosed | 3.22 |

## 3.3 Water Test Rig II

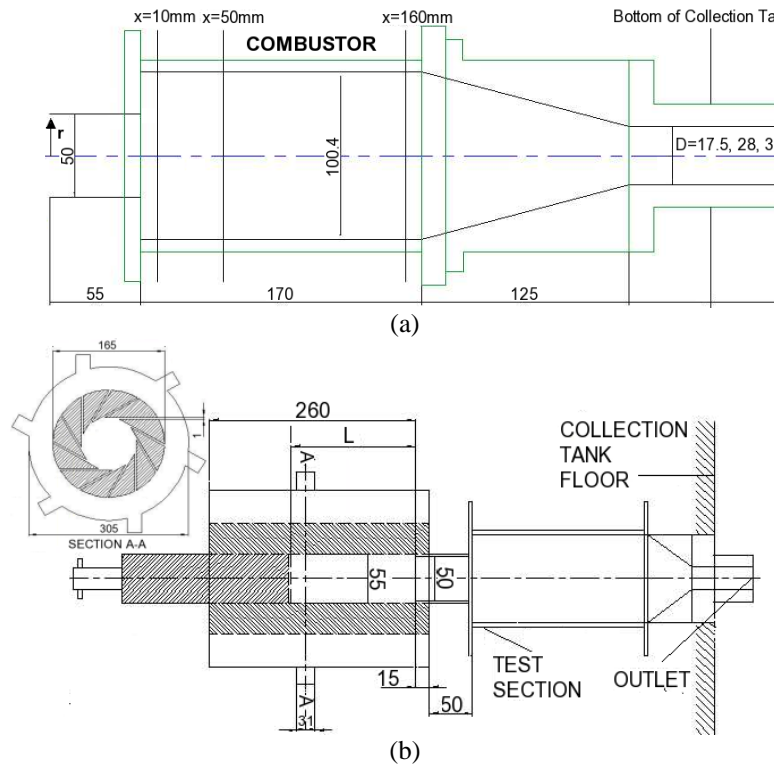A sketch of the water flow model combustor can be seen in Fig. 5.



(a)



(b)

**Fig. 5** Water test rig II: (a) test combustor, (b) swirl generator.

The swirl generator is based upon the tangential-inlet design of Escudier et al. [23], but now using 12 narrow slits distributed uniformly around the axis. Measurements are carried out by LDA at three axial positions (Fig. 5). Different configurations are measured. The Reynolds number based on the combustor bulk axial velocity and diameter is about 2300, for all cases. The swirl level is characterized by the velocity ratio β, denoting the ratio of the slit exit velocity to the bulk axial combustor inlet velocity. The influence of exit diameter ($D_E$) is also investigated in the measurements. In the present work, the case with β=0.65 and $D_E$=35mm will be discussed.

The solution domain is defined to include the combustor and the swirl generator. Preliminary 3D RANS computations were performed for a domain covering the plenum and channels of the swirl generator to obtain the inlet conditions. For the main computations, the block-structured grid consisted of approximately 1,000,000 hexahedral finite volumes.

Instantaneous iso-surface of zero axial velocity predicted by URANS-RSM is presented in Fig. 6. URANS-RSM predicts a closed bubble in the combustor, and cannot capture any substantial flow transience for the investigated case, apart from time variations of negligible magnitude (thus, the time-averaged iso-surface is practically the same as the one shown in Fig. 6) .

Instantaneous and time-averaged contours of zero axial velocity predicted LES are presented in Fig. 7. One can see that transient, three-dimensional eddy structures are captured by the LES methodology (Fig. 7a). The time-averaged LES results (Fig. 7b) predict a recirculation bubble, which is closed on the downstream side, but extending upstream all the way through the swirl generator.

Predicted and measured traversal profiles of the time-averaged axial velocity component (u) at the axial measuring stations (Fig. 5a) at x=10mm, x=50mm and x=160mm are displayed in Fig. 8, which immediately reveal the complexity of the flow field (u and the traverse coordinate (y) are non-dimensionalized by bulk axial inlet $U_I$ and combustor radius R, respectively).

The experimental results show recirculation regions as well as on the axis, and in the corner downstream of the sudden expansion into the combustor, at the axial stations x=10mm and x=50mm. At x=160mm, it can be observed that both recirculation zones have disappeared, and, on the axis, the reverse flow zone is replaced by a strong jet-like overshoot.

At x=10mm, the characteristics of the time-averaged flow are captured very well by the LES. The URANS-RSM methodology can only roughly predict the qualitative behavior of the experimental results, showing large quantitative discrepancies to the latter.

At x=50mm, the LES comes again quite close to the experimental data and performs better than the URANS-RSM. However, the URANS-RSM predictions for x=50mm show a better agreement with the experiments than they do for x=10mm.

At x=160mm, the quantitative agreement of the LES with the experimental data is not very well, as the LES underpredicts the maximum axial velocity on the axis. Nevertheless, the LES still shows a qualitative agreement with the experiments, whereas URANS-RSM cannot capture the flow features even qualitatively.

Predicted and measured traversal profiles of the time-averaged swirl velocity component (w) at the axial measuring stations (Fig. 5b) at x=10mm, x=50mm and x=160mm are displayed in Fig. 9 (w and the traverse coordinate (y) are non-dimensionalized by bulk axial inlet $U_I$ and combustor radius R, respectively).

The experimental data shows a forced-vortex-like region in the vicinity of the axis, changing over to a free-vortex-like distribution at higher values of the radial coordinate. It is interesting to note that the vortex core first radially expands between the stations x=10mm and x=50mm, and then contracts between x=50mm and x=160mm. This is accompanied by the corresponding decreases and increases of the swirl velocity gradients and the peak swirl velocities near the axis.

For the time-averaged swirl velocity component, the LES predictions at the stations x=10mm and x=50mm agree quite well with the experimental data, whereas URANS-RSM performs again rather poorly. At x=160mm none of the both predictions agrees very well with the measurements. However, the LES predictions are still much more satisfactory than URANS-RSM ones.
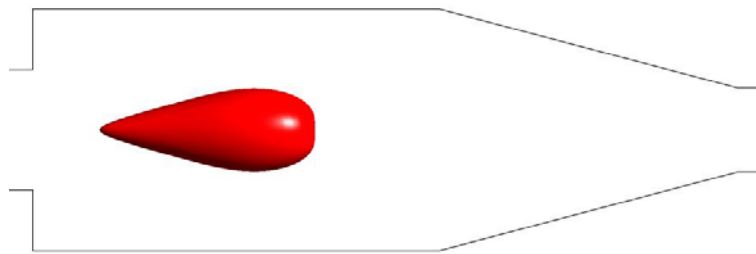


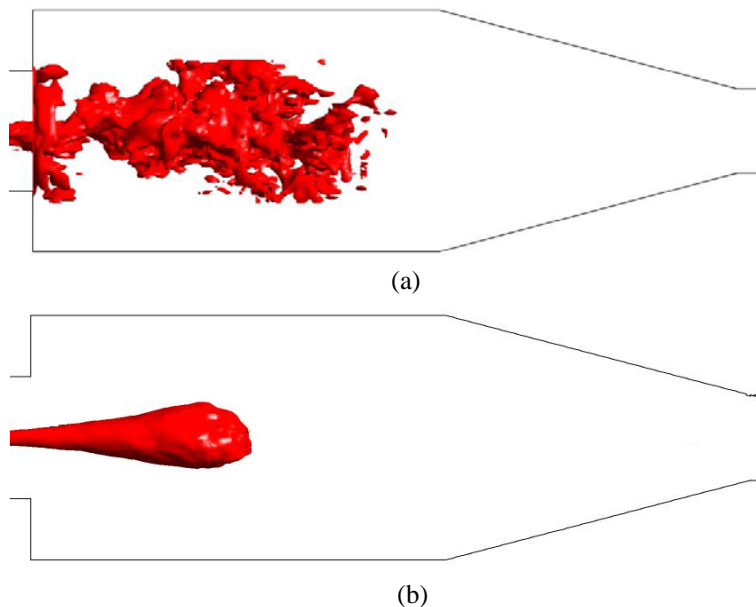**Fig. 6** Instantaneous iso-surface of zero axial velocity computed by URANS-RSM.



(a)



(b)

**Fig. 7** Iso-surfaces of zero axial velocity computed by LES: (a) instantaneous, (b) time-averaged.
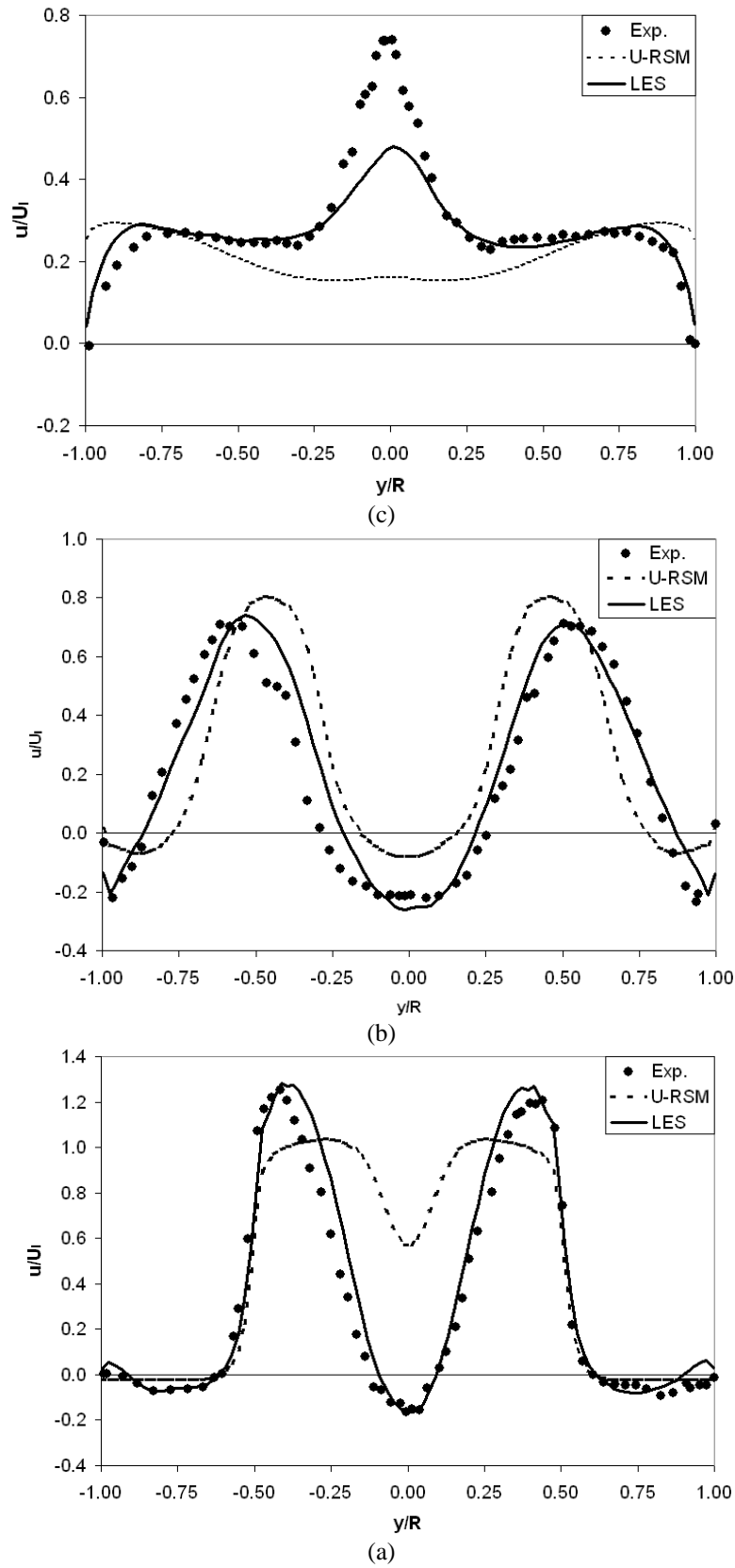
**Fig. 8** Time-averaged radial profiles of axial velocity component (u) at (a) x=10mm, (b) x=50mm, (c) x=160mm.

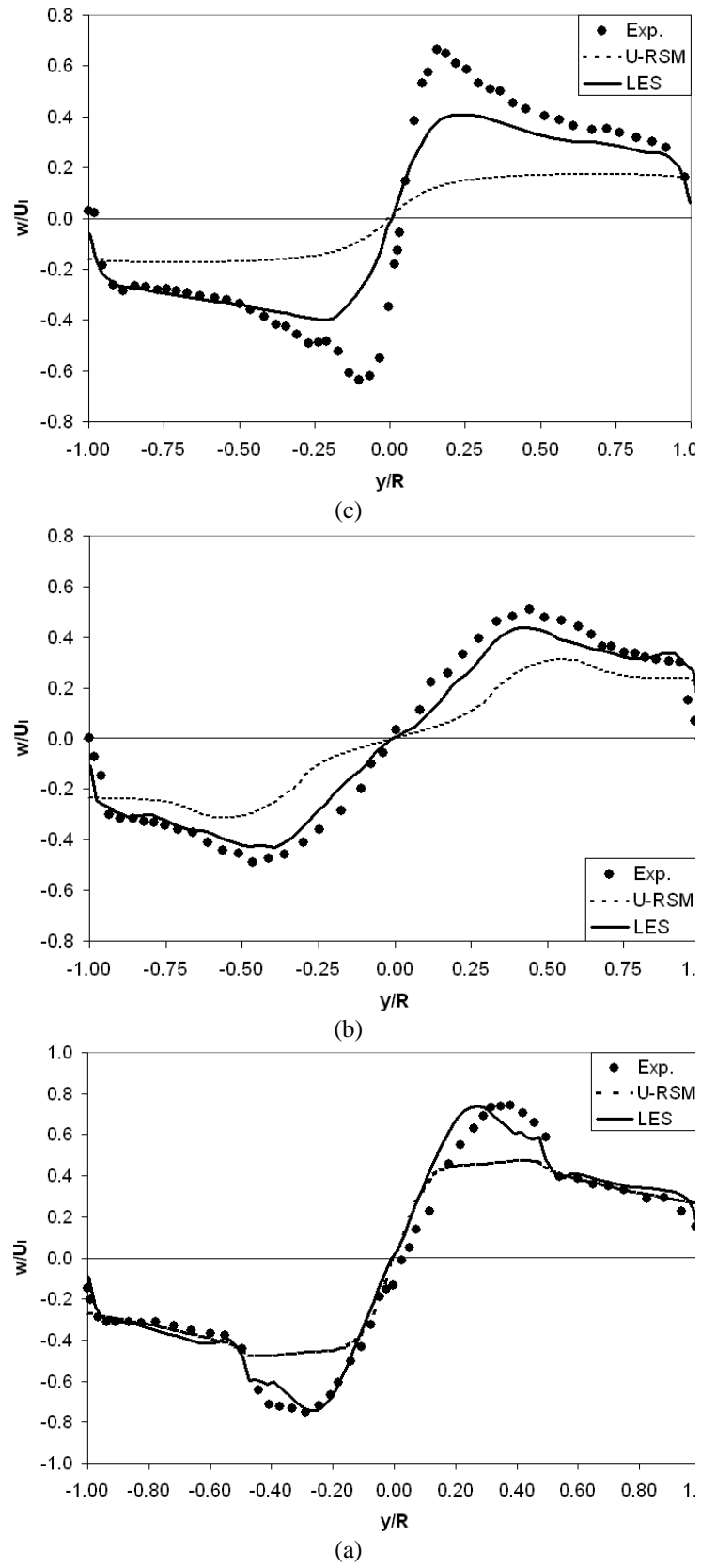**Fig. 9** Time-averaged radial profiles of swirl velocity component (w) at (a) x=10mm, (b) x=50mm, (c) x=160mm.

## 4. Conclusion

Turbulent swirling flows in gas turbine configurations have been investigated for a combusting flow in an industrial test rig and isothermal flow in two different water test rigs. The URANS-RSM was applied to all of the cases. For the industrial test rig, the URANS-RSM was observed to deliver a very good qualitative agreement with the experimental observations. For the first water test rig, a good agreement of the URANS-RSM with the experiments was observed, again. However, the performance of the URANS-RSM for the second water test rig was observed to be rather poor. This is expected to be caused by the quite low Reynolds number of the rig, since the applied RSM formulation has been a high Reynolds number one. The LES was applied to the both water test rigs. The agreement of the LES with the experiments was observed to be very good for the second test rig, which is expected to be due due to a very good resolution of the turbulent length scales by the underlying grid at this low Reynolds number. The performance of the LES for the first water test rig was poor, which is expected to be caused by an insufficient resolution of the turbulent length scales by the existing grid, at the comparably higher Reynolds number of the rig. The DES, which was applied to the first water test rig only, has shown the best agreement with the experiments for that rig.

## References

[1] Cramb, D. J. and McMillan, R., 2001, "Tempest Dual Fuel DLE Development and Commercial Operating Experience and Ultra Low NOx Gas Operation", ASME Paper 2001-GT-76.

[2] Escudier, M. and Keller, J. J., 1983, "Vortex Breakdown: A Two Stage Transition", Aerodynamics of Vortical Type Flows in Three Dimensions", AGARD CP No. 342, Paper No. 25.

[3] Weber, R., Boysan, F., Swithenbank, J. and Roberts, P. A., 1986, "Computation of Near Field Aerodynamics of Swirling Expanding Flows', Proc. 21st Symp. (Int.) Combustion, The Combustion Institute, Pittsburgh, pp. 1435-1443.

[4] Hogg, S. and Leschziner, 1988, "Computation of Highly Swirling Confined Flow with a Reynolds Stress Turbulence Model', AIAA Journal, Vol. 27, pp. 57-63.

[5] Benim, A. C., 1990, "Finite Element Analysis of Confined Swirling Flows", International Journal for Numerical Methods in Fluids, Vol. 11, pp. 697-717.

[6] Spall, R. E. and Gatski, T. B., 1995, "Numerical Calculations of 3D Turbulent Vortex Breakdown", International Journal for Numerical Methods in Fluids, Vol. 20, pp. 307-318.

[7] Turrell, M. D., Stopford, P. J., Syed, K. J. and Buchanan, E., 2004, "CFD Simulation of the Flow within and Downstream of a High-Swirl Lean Premixed Gas Turbine Combustor", ASME Paper GT2004-53112.

[8] ANSYS-CFX-10, 2006, "SolverManual", ANSYS Inc.

[9] Sloan, D. G., Smith, P. J. and Smoot, L. D., 1986, "Modelling of Swirl in Turbulent Flow Systems", Progress in Energy and Combustion Science, Vol. 12, pp. 163-250.

[10] Launder, B. E., Reece, G. J. and Rodi, W., 1975, "Progress in the Development of a Reynolds-Stress Turbulence Closure", Journal of Fluid Mechanics, Vol. 68, pp. 537-566.

[11] Speziale, C. G., Sarkar S. and Gatski, T. B., 1991, "Modelling the Pressure-Strain Correlation of Turbulence", Journal of Fluid Mechanics, Vol. 227, pp. 245-272.

[12] Sagaut, P., 2002, Large Eddy Simulation for Incompressible Flows – An Introduction, 2nd Ed., Springer, Berlin.

[13] Smagorinsky, J., 1963, "General Circulation Experiments With the Primitive Equations. I: The Basic Experiment". Monthly Weather Review, Vol. 91, pp. 99-164.

[14] Hinze, J. O., 1959, Turbulence, McGraw-Hill, New York.

[15] Travin, A., Shur, M., Strelets, M. and Spalart, P., 1999, "Detached-Eddy Simulations Past a Circular Cylinder", Flow, Turbulence and Combustion, Vol. 63, pp. 293-313.

[16] Strelets, M., 2001, "Detached Eddy Simulation of Massively Separated Flows", AIAA Paper 2001-0879.

[17] Menter, F. R., 1994, "Two Equation Eddy-Viscosity Turbulence Models for Engineering Applications", AIAA Journal, Vol. 32, pp. 1598-1695.

[18] Magnussen, B. and Hjertager, B., 1976, "On Mathematical Modelling of Turbulent Combustion with Special Emphasis on Soot Formation and Combustion", Proc. 16th Symp. (Int.) Combustion, The Combustion Institute, Pittsburgh, pp. 719-729.

[19] Westbrook, C. and Dryer, H., 1981, "Simplified Reaction Mechanisms for the Oxidation of Hydrocarbon Fuels in Flames", Combustion Science and Technology, Vol. 2, pp. 31-47.

[20] Bradshaw, P. (Ed.), 1978, Turbulence, Springer, Berlin.

[21] Peyret, R (Ed.), 2000, Handbook of Computational Fluid Mechanics, Academic Press, San Diego.

[22] Escudier, M. P. and Keller, J. J., 1985, "Recirculation in Swirling Flow: A Manifestation of Vortex Breakdown", AIAA Journal, Vol. 23, pp. 111-116.

[23] Escudier, M. P., Bornstein, J. and Zehnder, N., 1980, "Observations and LDA Measurements of Confined Turbulent Vortex Flow", Journal of Fluid Mechanics, Vol. 98, pp. 490-463.